Research on the Tensile Strength and Properties of Anchored Layered Composite Rock

Zhongyi He *, Yongsheng Liu, Zhijie You

East China Jiaotong University, Nanchang, Jiangxi, 330013, China

*1377350349@qq.com

Abstract. I used Why-3000 compression servo testing device to do experiments about rock specimens fixed on different angle inclinations. This study systematically analyzed tensile mechanical property of layered rocks with different anchoring configurations at varied dip angle, experimental results show, under unanchored condition, the stress-radial straing curves of specimens exhibited monotonically decreasing trends in all dip angle (0-90) and both tensile strength and strain reached minimum value at 90°dip angle. Anchored and pre-strengthened samples had far greater tensile strength and radial strain than unanchored samples, and with much lower rates of strain increase. To show that rock bolts accomplish complete improvement of bearing capacity by controlling rock mass deformation and altering stress distribution. Watching the same condition of stratigraphic dip angle, preload stress. The tensile strength and radial strain level of the zero degree-anchoringangle specimen is much higher than the 15 degree-anchoring-specimen: It implies that good anchorage angles could take charge of rock mass bearing ability evolution processes because of better stress transition ways and more deformation limitation results.

Keywords: Anchored layered rock; Brazilian split test; Radial strain; Tensile strength

1 Introduction

Considering the complex geological conditions of underground works, increasing excavation depth, etc., many scholars come up with new bolt systems, for example, inflatable bolts [1].In addition, due to the multitude of parameters affecting the performance of bolt anchorage, many researchers have conducted extensive experimental and numerical research on important parameters such as bolt diameter[2] and bolt/cable eccentricity[3], providing useful knowledge for optimizing anchorage effect; Jiang et al. [4] prepared and tested various artificial rock joint specimens with different strength grades and studied their macroscopic shear strength, failure mode and meso-scale microcrack development. Grindheim et al. [5] conduct full-scale pull-out tests on rock anchors in a limestone quarry. They investigate the bond failure condition at the anchor-grout and grout-rock interfaces. They showed that rock strength controls joint shear behavior, with stronger joints having higher shear strength and more brittle failure, and

S. Sing et al. (eds.), *Proceedings of the 2025 7th International Conference on Civil Architecture and Urban Engineering (ICCAUE 2025)*, Atlantis Highlights in Engineering 43,
https://doi.org/10.2991/978-94-6239-682-1_9

weaker joints having less shear strength and more progressive microcrack growth. Their work made it clear the unique failure methods and bond performance distinctions between those two interfaces. Wu et al. [6] did experimentation that looked into how joint roughness together with infill thinness changed rock mass shear traits, finding how these shaped shear strength and also failure forms. Song et al.[7]used 3D particle-based numerical simulations to figure out sandstone's mechanical reactions under multiple-level compressive difference cyclic loading (DCL), making clear its damage development traits and distortion aspects.

2 Specimen Preparation and Loading Scheme

Specimen Preparation: Standard cylindrical red sandstone specimen (50mm×25mm, height×diameter)were used. They were cut symmetrically from base rock along four directions (0°, 30°, 60°, 90°)relative to the central short axis via a single-blade saw, then had end faces ground to standard on a double-end grinder. Symmetric layers were bonded with dolomite adhesive, and samples stored cool/dry for ~1 week.For tests, anchorage angles (0°/15°) were set. A 2 mm-diameter screw (433 MPa tensile strength) acted as the simulated bolt. Based on bedding angle analysis, 3 mm-diameter holes were drilled along a 0°/30°/60°/90° reference line. A composite grout (epoxy+polyamide resins+ anhydrous ethanol) was mixed; after grouting, the bolt was inserted. A 0.5 N/m preload was finally applied with a torque wrench to mimic field conditions.Fig. 1 shows anchored specimen diagrams by bedding angle; Table 1 lists sample IDs.

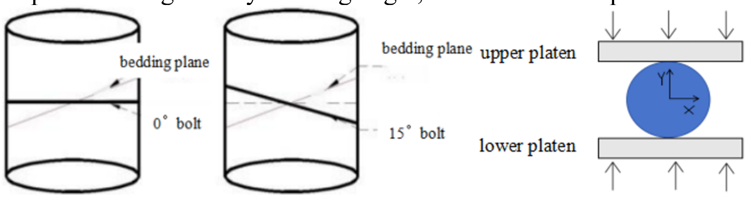

Note: α=0°, 30°, 60°, 90° Simplified Test Diagram of Rock Sample

Fig. 1. Figures of Anchored Rock Specimens with Different Beddings

Table 1. Specimen numbering for partial rock specimens in the Brazilian splitting test

Specimen Identification Number	Designation
B-1, B-2, B-3	Single intact rock specimen
BW-0-1, BW-0-2, BW-0-3	unanchored rock specimen with 0° bedding
BN0-0-1, BN0-0-2, BN0-0-3	0° anchored rock specimen with 0° bedding and no pre-tightening force

B—Brazilian splitting test, W—No anchoring, N—No preload force, F—Has preload force

3 Experimental Results and Analysis

3.1 Test Results of Rock Samples Without Anchor

As shown in Fig.2, during initial loading, contact with the loading plates at both ends induces local compressive deformation, with the curve exhibiting a nonlinear upward trend. As voids gradually close, the curve transitions to linear growth. Under further loading, cracks initiate and coalesce in the interior and near bedding planes, eventually causing rock fracture and a sudden stress drop.

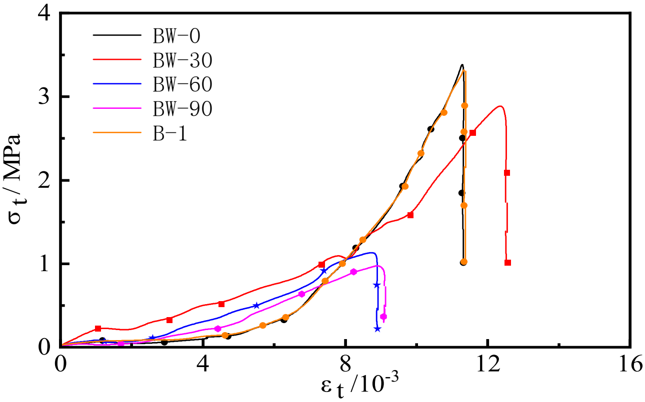

Fig. 2. Stress-strain curve of non-bedded or massive rock specimens

3.2 The Results of the Anchor Rock Sample Test

Fig.3 shows stress-strain curves for anchored bedded rock specimens. Their behavior differs markedly from intact rock and unanchored counterparts: Shortly after contacting loading platens, localized compaction deformation occurred at the ends—with the bolt unloaded—causing nonlinear initial rise. Once voids compacted, rock-bolt coordinated deformation began, linearizing the curve. Under sustained loading, new cracks nucleated near bedding, but bolt constraint slowed fracture—manifesting as serrated fluctuations and residual strain. Eventually, crack coalescence triggered sudden stress drop and failure.

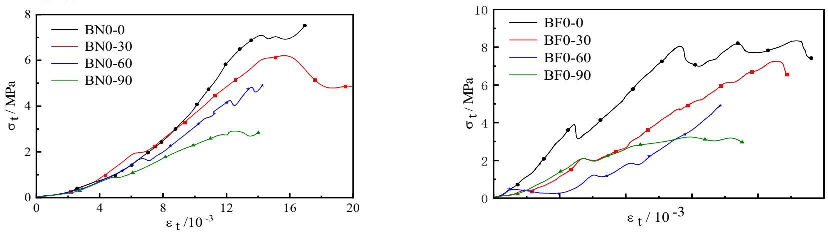

(a) 0° with anchor without preload force

(b) 0° anchor has preload force

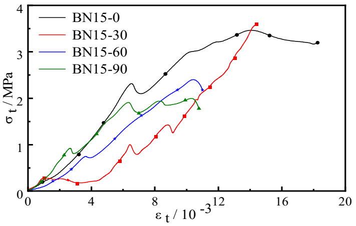

(c) 15° with anchor without preload force

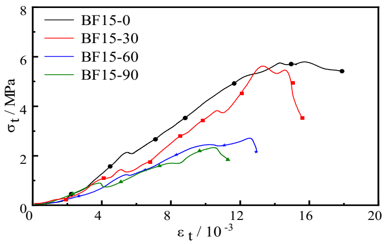

(d) 15° with anchor has preload force

Fig. 3. Anchored stratified rock stress-strain curve

3.3 Analysis of Test Results

The influence of preload force. Fig.4 presents stress-preload curves for anchored bedded rock specimens. Subfigure (a): Peak stress increase from unanchored → non-preloaded → preloaded was minimal at 0° bedding and maximal at 60°.Subfigure (b): The increase stayed minimal at 0° and peaked at 30°.At 0°, tensile strength peaks (bedding planes vertical), but limited bolt displacement constraint yields the smallest anchorage-induced stress rise. At 30°/60°, specimens tend to shear fail—here, the bolt restricts radial displacement and applies preload, inhibiting shear displacement and thus maximizing stress increase amplitude.

The influence of anchoring angle. Fig.5 presents preload-stress curves for anchored bedded rock. Compressive strength improved notably across 0°–90°. At 0° bedding, total stress increase varied minimally between non-preloaded and preloaded states; at 60°, it was maximal. This disparity arises from higher shear stresses at 60°: the bolt aligns with the bedding plane, enhancing anchorage force transfer to the loaded face. At 0°, the rock's tensile strength peaks (with its tensile plane perpendicular to bedding), leading to a smaller stress rise.

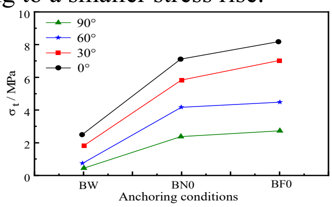

(a) The influence of 0° anchor preload force on the stress changes of bedding rocks

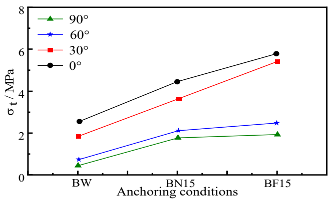

(b) The influence of 15° anchoring preload force on the stress changes of bedding rocks

Fig. 4. Anchored layered rock stress-preload curve

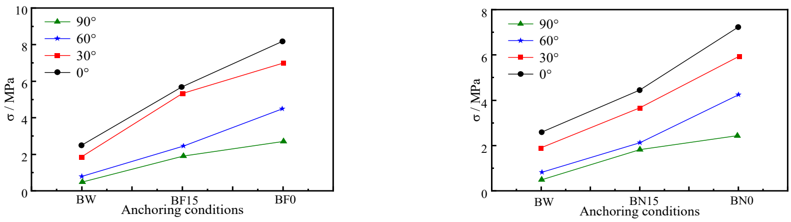

(a) The stress variation patterns of layered rocks under different anchoring angles under the action of preload force

(b) Study on Stress Changes in Stratified Rock with Different Anchoring Angles under No Tension Force Conditions

Fig. 5. Anchored layered rock preload-stress relationship curve

The influence of the bedding angle of rock samples. Fig.6 shows the stress - strain curves of the anchored rock samples and the correlation between bedding inclination and stress/strain. Fig.6 (a): Tensile strength decreases linearly with the increase of bedding inclination. Under all anchorage conditions, stress (0°-90°): BN15 < BF15 < BN0 < BF0. It implies bolts improve tensile performance at (0°>15°). Preload also increases strength - this shows that the combination of bolt angle and preload works well to make the rock mass stronger. Subfigure (b): Subfigure (b) Strain decreases linearly as bedding inclines. In all conditions, the order of the strain(0°–90°) was the same: BN15 < BF15 < BN0 < BF0. To show that bolts improve tensile performance and deformation resistance at 0 > 15, and that preload increases strain.

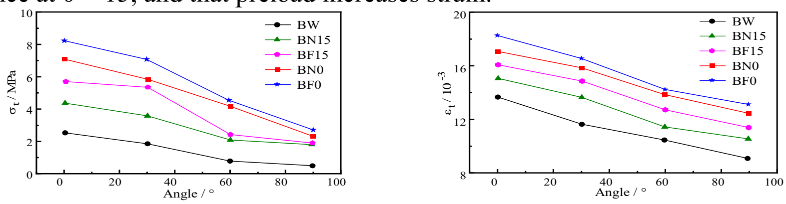

(a) Inclination-stress curve

(b) Inclination-strain curve

Fig. 6. Unanchored layered-rock stress-strain curve

Analysis of anchoring mechanism. When a bolt goes into layered rock, this creates a bond between the rock-anchor and the part that gets stronger when there's an anchor there. But the others, which are the sides perpendicular to the bolt face laterally, are still susceptible to failure. Upper/ lower secondary stress superposition zones improve beds dips impact and ease of structural faults. Mechanical large beddings cause slip failures of rock-anchor composite and contacts planes. With strong and sufficient bolt support and high bonding strength between the two parts, the brittle crushing area of the bolt first forms tensile-shear cracks under axial force loading - finally resulting in composite failure.

4 Analysis of Deviant Forms

4.1 Analysis of Rock Sample Failure Under External Force

Fig. 7 shows the failure morphology of bedded rock specimens with anchoring angles of 0° and 15°.Subfigure (a): At 0°/90° the rock failed in a central tension failure mode with one through crack (no secondary cracks present)—the bolt is inhibiting the crack from propagating. At this frequency there were many secondary cracks occurring at the loaded ends now cracking planes started to connect. At 60°, end cracks lead to final through-tensile failure, both stress distribution and failure modes are modified. Subfigure (b) shows that preload prevented cracking: compared to the 0 preload specimen, the number of crack at 30/90 is lower. At 60°, it also prevented cracks from reaching the midsection. Subfigure (c) shows: 0°/90° still failed central, cracks diverted towards the bolt to create crescents. At 30°, cracks extended curvilinearly. Replacing it at 60°, because the bolt was inhibited from failure and it caused through tensile and bedding-parallel shear slip cracks, which shows a 0 degree' s performance is superior over 15 degree for tensile/crack Subfigure (d): 0°/90°failed centrally then crack deflection into crescents. At 30°, cracks extended curvilinearly. At 60degrees it failed to prevent throughcracks and shear slip cracks. 0° samples were better than 15° samples in tensile/crack resistance.

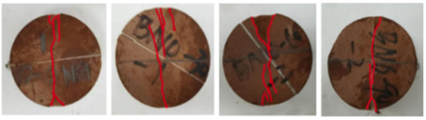

(a) A 0°-degree inclined rock sample with no pre-tightening layering force Failure Mode.

(b) The 0°anchor - preloaded layered rock sample's failure morphology

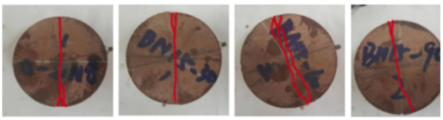

(c) A 15°-degree inclined rock sample with no pre-tightening layering force Failure Mode.

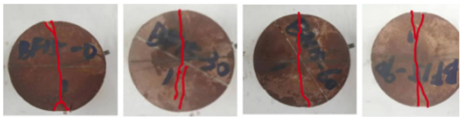

(d)The 15°anchor - preloaded layered rock sample's failure morphology

Fig. 7. Fracture patterns of anchored bedding rock specimens at 0° and 15° orientations

5 Conclusion

1) All specimens display monotonically decreasing stress-radial strain curves over the 0°–90° range. At a 90° inclination angle, both tensile strength and strain attain their minimum values.

2) Under the condition of 0°bolt installation angle and 60° bedding dip angle, the rock specimenunderwent a sequential transition: unbolted → bolted without pretension → bolted with pretension. Peak stress growth rates for these steps were 263% and 6%, respectively, representing an overall increase of 285% from the initial unbolted state.

For the 15° bolt installation angle with a 30° bedding dip angle, the specimen followed the same progression, yielding peak stress growth rates of 73% and 43%, and an overall enhancement of 148%.

3) Under identical bedding dip angles and pretension forces, specimens with a 0° bolt installation angle exhibited higher tensile strength and strain than those with a 15° angle. This indicates that an appropriate bolt installation angle can dominate the evolution of the rock mass's bearing capacity by optimizing stress transfer paths and enhancing deformation constraint effects.

References

1. LI C C, AURE A, KNOX G. Experimental study of the effects of borehole size, borehole roughness, and installation pressure on the pull load capacity of inflatable rockbolts[J].Rock Mechanics and Rock Engineering, 56: 8415-8431(2023)
2. FAN J Q,SHI X Y, KONG F L, et al, Calculation method of the effective anchorage length of anchorage structures based on analysis of the ultimate bearing capacity[J].Geotechnical & Geological Engineering, 39:4205-4212(2021)
3. HE D Y, LIU S W, JIA H S, et al. Anchoring eccentricity features and rectifying devices for resin grouted bolt/cable bolt[J]. International Journal of Mining Science and Technology, **32**(5): 1059-1073(2022)
4. JIANG Y J, ZHANG S H, LUAN H J, et al. Study on the effect ofrock strength on the macro-meso shear behaviors of artificial rockjoints[J].Geofluids, 2022: 1-15(2022)
5. GRINDHEIM B, LI C, HØIEN A.Full-scale pullout tests of rockanchors in a limestone quarry focusing on bond failure at the anchor-grout and grout-rock interfaces[J]. Journal of Rock Mechanics and Geotechnical Engineering, **15**(9): 2264-2279(2023)
6. WU X Z, ZHENG H F, WANG G, et al.Effect of Joint roughness andinfill thickness on shear characteristics of rock mass[J]. Advances inCivil Engineering,2022:1-12(2022)
7. SONG Z Y, YANG Z, ZHANG M, et al. Numerical characterizationof sandstone's mechanical responses under multi-level compressivedifferential cyclic loading(DCL): A 3D particle-based numerical investigation[J].Computers and Geotechnics,154: 105109(2023)